

Vibrational study and thermal behavior of dihydrogenotriphosphate trihydrate of 4-aminobenzoic acid and its anhydrous new form fertilizer type NP

Mustapha Belhabra ^{1,*}, Ismail Fahim ¹, Azzedine Atibi ^{1,2}, Khadija El Kababi ^{1,2}, Ali Ouasri ³, Soufiane Zerraf ¹, Malika Tridane ^{1,2}, Mohammed Radid ¹, and Said Belaouad ¹

¹ Laboratoire de Chimie Physique des Matériaux LCPM, Faculté des Sciences Ben M'sik, B. P. 7955. Bd Cdt Driss El Harti. Université Hassan II de Casablanca, Maroc

² Centre Régional des métiers d'éducation et de formation Casablanca Anfa, Bd Bir Anzarane Casablanca, Maroc

³ Centre Régional des métiers d'éducation et de formation Rabat. Maroc

Abstract: Chemical synthesis methods and IR spectrometry studies are reported for an organic triphosphate $(\text{NH}_3\text{C}_6\text{H}_4\text{COOH})_3\text{H}_2\text{P}_3\text{O}_{10}\cdot 3\text{H}_2\text{O}$ and its anhydrous new form $\text{NH}_3\text{C}_6\text{H}_4\text{COOH})_3\text{H}_2\text{P}_3\text{O}_{10}$. The hydrate compound $(\text{NH}_3\text{C}_6\text{H}_4\text{COOH})_3\text{H}_2\text{P}_3\text{O}_{10}\cdot 3\text{H}_2\text{O}$ was synthesized by the ion-exchange resin method. The dehydration of $(\text{NH}_3\text{C}_6\text{H}_4\text{COOH})_3\text{H}_2\text{P}_3\text{O}_{10}\cdot 3\text{H}_2\text{O}$ leads at 130°C to $(\text{NH}_3\text{C}_6\text{H}_4\text{COOH})_3\text{H}_2\text{P}_3\text{O}_{10}$ crystallizing in the triclinic system with space group P 1 ($Z = 2$) [$a = 14.566(6)$ Å, $b = 6.866(1)$ Å, $c = 6.445(6)$ Å, $\alpha = 112.36(3)^\circ$, $\beta = 94.51(1)^\circ$, $\gamma = 95.94(7)^\circ$, and $V = 587.98(1)$ Å³]. Merit's figures are $M(10) = 91.9$ and $F(10) = 55.6(0.0032, 56)$. Its thermal behavior and kinetic study were studied by using thermal analyses TGA and DTA techniques between 25 and 600°C.

Keywords: *p*-carboxyphenylammonium triphosphate; IR spectrometry; vibrational study; thermogravimetric and differential analyses (TGA–DTA); Kinetic; Ozawa; KAS.

Introduction

The *p*-carboxyphenylamine (4-aminobenzoic acid) considered as a biological molecule, has an anticoagulant and antioxidant properties. It exists naturally in foods; it is produced by essential symbiotic bacteria to metabolize constantly in the human body ¹. The active sites of several biological systems have kind of hydrogen bonding in hybrid compound ². Indeed, the crystal structures of 4-carboxyphenylammonium dihydrogen phosphate and 4-carboxyanilinium hydrogen sulphate compounds have been recently studied ^{3,4}. Furtherer, the *p*-carboxyphenylammonium dihydrogen-monophosphate monohydrate compound was found to consist of H_2PO_4^- anions, water molecules and *p*- $\text{HOOC-C}_6\text{H}_4\text{-NH}_3^+$ cations ⁵. In this structure, anions and cations are linked to each other through strong hydrogen bonds, formed by all H atoms covalently bonded to anions, nitrogen, carboxylic groups and water molecules. A three-dimensional complex network of hydrogen bonds ensures the cohesion of the ionic structure.

The literature contains numerous studies of solid materials containing the P_3O_{10} group like $\text{NH}_4\text{ErHP}_3\text{O}_{10}$, $\text{CuNa}_3\text{P}_3\text{O}_{10}\cdot 12\text{H}_2\text{O}$, $\text{CuNa}_3\text{P}_3\text{O}_{10}$, $\text{MgNa}_3\text{P}_3\text{O}_{10}\cdot 12\text{H}_2\text{O}$, $\text{MgNa}_3\text{P}_3\text{O}_{10}$, $\text{NiNa}_3\text{P}_3\text{O}_{10}\cdot 12\text{H}_2\text{O}$ et $\text{NiNa}_3\text{P}_3\text{O}_{10}$ ⁶⁻¹⁰. During a systematic investigation of triphosphates associated with organic matrixes, the triphosphate trihydrate of para carboxyphenylammonium $(\text{NH}_3\text{C}_6\text{H}_4\text{COOH})_3\text{H}_2\text{P}_3\text{O}_{10}\cdot 3\text{H}_2\text{O}$ was prepared by the method of ion-exchange resin ¹¹ in our laboratory ^{12,13}.

The present study reports on the chemical preparation, IR vibrational spectroscopy, thermal dehydration and decomposition by thermal analyses (TGA and DTA) of $(\text{NH}_3\text{C}_6\text{H}_4\text{COOH})_3\text{H}_2\text{P}_3\text{O}_{10}\cdot 3\text{H}_2\text{O}$. The total thermal dehydration of this compound leads to the corresponding anhydrous form, which is a new triphosphate of para carboxyphenylammonium $(\text{NH}_3\text{C}_6\text{H}_4\text{COOH})_3\text{H}_2\text{P}_3\text{O}_{10}$. The kinetic parameters of dehydration have been studied for the title compound. Indeed, $(\text{NH}_3\text{C}_6\text{H}_4\text{COOH})_3\text{H}_2\text{P}_3\text{O}_{10}\cdot 3\text{H}_2\text{O}$

and $(\text{NH}_3\text{C}_6\text{H}_4\text{COOH})_3\text{H}_2\text{P}_3\text{O}_{10}$ are binary organic fertilizers type NP (nitrogen and phosphorus) second generation and corrosion inhibitors¹⁴⁻¹⁵. The two triphosphates associated with para carboxyphenylammonium reported in the present work are stable in the normal conditions of temperature and hygrometry.

Experimental



The so-obtained solution was then slowly evaporated at room temperature until large prisms of $(\text{NH}_3\text{C}_6\text{H}_4\text{COOH})_3\text{H}_2\text{P}_3\text{O}_{10}.3\text{H}_2\text{O}$ were obtained. The triphosphoric acid, $\text{H}_5\text{P}_3\text{O}_{10}$, used in this reaction was prepared from an aqueous solution of $\text{Na}_5\text{P}_3\text{O}_{10}$ passed through an ion-exchange resin 'Amberlite IR120'¹¹. $(\text{NH}_3\text{C}_6\text{H}_4\text{COOH})_3\text{H}_2\text{P}_3\text{O}_{10}.3\text{H}_2\text{O}$ is stable in the normal conditions of temperature and hygrometry. $(\text{NH}_3\text{C}_6\text{H}_4\text{COOH})_3\text{H}_2\text{P}_3\text{O}_{10}.3\text{H}_2\text{O}$ was



$(\text{NH}_3\text{C}_6\text{H}_4\text{COOH})_3\text{H}_2\text{P}_3\text{O}_{10}$ is stable in the normal conditions of temperature and hygrometry.

With the additional increase in temperature, $(\text{NH}_3\text{C}_6\text{H}_4\text{COOH})_3\text{H}_2\text{P}_3\text{O}_{10}$ is decomposed by evolving NH_3 followed by CO_2 .

Data Collection and Reduction

Thermal behavior. Coupled TGA-DTA thermal analyses were performed using the multimodule 92 Setaram Analyzer operating from room temperature up to 1400°C, in a platinum crucible, at various heating rates from 1 to 15°C/min.

Infrared spectrometry. The infrared spectra of the powdered samples of $(\text{NH}_3\text{C}_6\text{H}_4\text{COOH})_3\text{H}_2\text{P}_3\text{O}_{10}.3\text{H}_2\text{O}$ and $(\text{NH}_3\text{C}_6\text{H}_4\text{COOH})_3\text{H}_2\text{P}_3\text{O}_{10}$ were recorded in the range 4000-400 cm^{-1} with a Perkin-Elmer IR 983G spectrophotometer, using samples dispersed in spectroscopically pure KBr pellets.

Results and Discussion

Crystallographic Characterization

- $(\text{NH}_3\text{C}_6\text{H}_4\text{COOH})_3\text{H}_2\text{P}_3\text{O}_{10}.3\text{H}_2\text{O}$

$(\text{NH}_3\text{C}_6\text{H}_4\text{COOH})_3\text{H}_2\text{P}_3\text{O}_{10}.3\text{H}_2\text{O}$ studied elsewhere^{12,13} crystallizes in the triclinic system with space group $\text{P}\bar{1}$ ($Z = 2$) [$a = 9.844(1)$ Å, $b = 13.086(4)$ Å, $c = 13.320(2)$ Å; $\alpha = 107.12(2)^\circ$, $\beta = 106.08(1)^\circ$, $\gamma = 97.87(2)^\circ$, and $V = 1530(1)$ Å³].

Synthesis $(\text{NH}_3\text{C}_6\text{H}_4\text{COOH})_3\text{H}_2\text{P}_3\text{O}_{10}.3\text{H}_2\text{O}$

Single crystals of $(\text{NH}_3\text{C}_6\text{H}_4\text{COOH})_3\text{H}_2\text{P}_3\text{O}_{10}.3\text{H}_2\text{O}$ were prepared by slowly adding dilute cyclotriphosphoric acid, $\text{H}_5\text{P}_3\text{O}_{10}$, to an aqueous solution of para carboxyphenylammonium, $\text{NH}_2\text{C}_6\text{H}_4\text{COOH}$ according to the following chemical reaction:

also obtained using the same method, by the hydrolysis of $\text{P}_3\text{O}_9^{3-}$ ion in aqueous solution $(\text{NH}_3\text{C}_6\text{H}_4\text{COOH})_3\text{H}_2\text{P}_3\text{O}_{10}$.

The product resulting from the total thermal dehydration of $(\text{NH}_3\text{C}_6\text{H}_4\text{COOH})_3\text{H}_2\text{P}_3\text{O}_{10}.3\text{H}_2\text{O}$, at 130°C, is a new anhydrous triphosphate of para carboxyphenylammonium $(\text{NH}_3\text{C}_6\text{H}_4\text{COOH})_3\text{H}_2\text{P}_3\text{O}_{10}$. The reaction is the following:

- $(\text{NH}_3\text{C}_6\text{H}_4\text{COOH})_3\text{H}_2\text{P}_3\text{O}_{10}$

$(\text{NH}_3\text{C}_6\text{H}_4\text{COOH})_3\text{H}_2\text{P}_3\text{O}_{10}$ crystallizes in the triclinic system with space group $\text{P}\bar{1}$ ($Z = 2$). Its unit-cell dimensions are: $a = 14.566(6)$ Å, $b = 6.866(1)$ Å, $c = 6.445(6)$ Å, $\alpha = 112.36(3)^\circ$, $\beta = 94.51(1)^\circ$, $\gamma = 95.94(7)^\circ$, and $V = 587.98(1)$ Å³. Merit's figures are $M(10) = 91.9$, and $F(10) = 55.6(0.0032, 56)$ ¹².

Vibrational study

Vibrations analysis of $\text{H}_2\text{P}_3\text{O}_{10}^{3-}$

The anion dihydrogenotriphosphate $(\text{H}_2\text{P}_3\text{O}_{10})^{3-}$ supposed to be of symmetry group C_1 , has 39 internal vibration modes [$\Gamma_{\text{int}} = 3 \text{ 9A}'$ (IR, Ra)]. According to this hypothesis, the anionic modes of $(\text{H}_2\text{P}_3\text{O}_{10})^{3-}$ free are all active in Raman and Infrared thus should appear in the form of simple bands.

In the structure of $(\text{NH}_3\text{C}_6\text{H}_4\text{COOH})_3\text{H}_2\text{P}_3\text{O}_{10}.3\text{H}_2\text{O}$, space group $\text{P}\bar{1}$ (Group of factors C_i)¹⁶, $(\text{H}_2\text{P}_3\text{O}_{10})^{3-}$ The anions have a C_1 site symmetry. This implies that all anionic internal modes (Table 1) generally remain infrared and Raman assets in the crystal site group. Theoretically, the presence of two units per unit of formula ($Z = 2$) doubles the number of cationic and anionic modes with Ag and Au symmetry in the group of factors C_i . In the crystal being centrosymmetric (C_i group factor), only Au insensitive augs are active in infrared. All modes of vibration are theoretically active in infrared and Raman. These anionic modes correspond mainly to the vibrations of the PO_4^{3-} and P-O-P.

Table 1. Correlation table ($C_1 \rightarrow C_i$) for the internal vibrational modes of $(H_2P_3O_{10})^{3-}$.

Point group : C_1	Site group : C_1	Factor group : C_i
39 A' (Ra, IR)	39 A' (Ra, IR)	39 A_g (Ra) 39 A_u (IR)

Vibrations analysis of 4-carboxyphenyl ammonium

The free 4-carboxyphenyl ammonium cation is assumed to be of C_s symmetry point group, and then has 48 internal vibrational modes described as $\Gamma_{int} = 32A'$ (IR, Ra) + 16 A'' (IR, Ra). According to this assumption, the cationic modes are all Raman and Infrared active and should appear as single bands. In the structure of $(NH_3C_6H_4COOH)_3H_2P_3O_{10} \cdot 3H_2O$ compound, of P1 space group (C_1 factor group) ¹⁶, 4-carboxyphenyl ammonium cations have C_1 site

symmetry. This implies that all cationic internal modes (Table 2) usually remain infrared and Raman actives in the site group of the crystal. The presence of two motifs per formula unit ($Z = 2$) doubles theoretically the number of cationic modes having A_g and A_u symmetry in the factor group C_i . It is concluded that all vibrational modes are theoretically Infrared and Raman active. Due to the centro symmetry of the crystal, only the ungerade modes A_u are Infrared active for the cations.

Table 2. Correlation table ($C_1 \rightarrow C_i$) for the internal vibrational modes of $(NH_3C_6H_4COOH)^+$.

Point group : C_1	Site group : C_1	Factor group : C_i
32 A' (Ra, IR)	32 A' (Ra, IR)	48 A_g (Ra)
16 A'' (Ra, IR)	16 A'' (Ra, IR)	48 A_u (IR)

The mainly crucial cationic vibration bands correspond principally to the vibrations of amino NH_3^+ , carboxyl groups and benzene ring. It is to note that the distribution of the internal vibrations modes for benzene group by developing the normal coordinate analysis has been carried out ¹⁷. In its free state, the NH_3^+ cation has C_{3v} symmetry with a pyramidal geometry; the corresponding normal vibrational modes are described as non-degenerate modes [$\nu_1(A_1)$, $\nu_2(A_1)$], and doubly degenerated [$\nu_3(E)$ and $\nu_4(E)$], which all active as well as in Raman and Infrared. In the 4-carboxyphenyl ammonium cation of C_s symmetry, all NH_3^+ modes become non-degenerate, with A' and A'' symmetry as indicated above, and usually remain Infrared and Raman active. The COOH has 9 internal vibrations modes given by $3m-3$, where m is the number of atoms in the group. These modes correspond to O-H stretching, C-O stretching, C=O stretching, in-plane-rocking, in-plane bending of C-O, in-plane bending of C=O, in-plane-bending of OH, out-of-plane wagging, and out-of-plane torsion.

Infrared Spectra of hydrate and anhydrous compounds

The infrared spectra of $(NH_3C_6H_4COOH)_3H_2P_3O_{10} \cdot 3H_2O$ and $(NH_3C_6H_4COOH)_3H_2P_3O_{10}$ compounds, recorded the range 4000–400 cm^{-1} , are given in Figures 1a and 1b. These compounds consist of NH_3^+ groups, COOH;

para-substituted benzene ring, $H_2P_3O_{10}$, and $3H_2O$ in the case of hydrate compound.

* NH_3^+ vibrations: Generally, the antisymmetric and symmetric stretching modes of the NH_3^+ group appear in the spectral region of 3200-2800 cm^{-1} spectral region; whereas the antisymmetric and symmetric deformations appear in the 1660-1610 cm^{-1} and 1550-1480 cm^{-1} regions, respectively. In the Infrared spectrum of the anhydrous compound, the $\nu_{as}(NH_3^+)$ stretching is observed as a medium band at 3230 cm^{-1} . The $\nu_s(NH_3^+)$ stretching modes give a weak and broad band at 2880 cm^{-1} in the case of the anhydrous compound and a medium band at 2887 cm^{-1} for the hydrated compound. The remaining bands corresponding to wagging $w(NH_3^+)$, twisting $t(NH_3^+)$ and rocking $\rho(NH_3^+)$ bending vibrations are assigned as indicated in Table 3.

* Carboxyl groups vibrations: Studying vibrational spectra of benzoic acid, Antony et al. ¹⁸ assigned C=O, C-O stretching modes; C-O, C=O in-plane bending, OH stretching, rocking mode, torsion mode and wagging mode to band appearing respectively at 1745 cm^{-1} , 1050 cm^{-1} , 594 cm^{-1} , 1804 cm^{-1} , 3785 cm^{-1} , 554 cm^{-1} , 594 cm^{-1} and 441 cm^{-1} . Florio et al. ¹⁹ observed C=O stretching at 1752 cm^{-1} , C-O stretching at 1347 cm^{-1} , C-O in-plane bending at 628 cm^{-1} , OH stretch at 3785 cm^{-1} , rocking mode at 628 cm^{-1} , and wagging mode at 160 cm^{-1} . In the present study, the assignment of bands corresponding to the different COOH vibrations is shown in Table 3.

* Para substituted benzene ring vibrations: The C-H stretching modes of benzene ring are generally expected in the 3115-3005 cm^{-1} ^{20, 21}. The $\beta(\text{C-H})$ "in-plane" and $\delta(\text{C-H})$ "out-plane" bending vibrations are located in the range 1250-1000 cm^{-1} and 900-690 cm^{-1} , respectively ^{21, 22}. For the studied compounds, the $\beta(\text{C-H})$ and $\delta(\text{C-H})$ of the benzene ring are observed in the expected ranges, as indicated in Table 3. The C=C and C-C benzene ring stretching modes occur in the 1650-1430 cm^{-1} and 1400-1300 cm^{-1} , respectively ^{20, 21}. For the two compounds, these modes are assigned to the corresponding bands as illustrated in Table 3. Finally, the C-N stretching and the ring breathing modes were identified for the studied compounds and given in Table 3.

* $\text{H}_2\text{P}_3\text{O}_{10}^{3-}$ vibrations: The assignment of bands due to the fundamental modes, valence and bending, of $\text{P}_3\text{O}_{10}^{5-}$ anions are presented in Table 3 for both triphosphates. The frequencies of the $\text{P}_3\text{O}_{10}^{5-}$ anion are assigned based on the characteristic vibrations of the P-O-P bridge, PO_2 and PO_3 groups. Since the P-O

bond in the PO_2 and PO_3 group is weaker than that in the

P-O-P Bridge, the vibrational frequencies of PO_2 and PO_3 are expected to be higher than those for P-O-P. The bands due to the symmetric and antisymmetric stretching frequencies of PO_2 and PO_3 in $\text{P}_3\text{O}_{10}^{5-}$ are generally observed in the region 1190-1010 cm^{-1} ^{22, 23}. The bands observed in the domain 970-840 cm^{-1} are attributed to the antisymmetric and symmetric POP stretching modes. The bands due to $\delta(\text{OPO})$, $\delta(\text{PO}_2)$, $\delta(\text{PO}_3)$ and $\delta(\text{POP})$ are also identified in Table 3, which contains the IR frequencies and the vibrational modes corresponding to $\text{Rb}_3\text{H}_2\text{P}_3\text{O}_{10} \cdot 1,5\text{H}_2\text{O}$, para-carboxyphenylammonium $\text{NH}_2\text{C}_6\text{H}_4\text{COOH}$, compared with those of $(\text{NH}_3\text{C}_6\text{H}_4\text{COOH})_3\text{H}_2\text{P}_3\text{O}_{10} \cdot 3\text{H}_2\text{O}$ and $(\text{NH}_3\text{C}_6\text{H}_4\text{COOH})_3\text{H}_2\text{P}_3\text{O}_{10}$. The IR frequencies of the $\text{P}_3\text{O}_{10}^{5-}$ anions observed in the two triphosphates associated to para carboxyphenylammonium, $(\text{NH}_3\text{C}_6\text{H}_4\text{COOH})_3\text{H}_2\text{P}_3\text{O}_{10} \cdot 3\text{H}_2\text{O}$ and $(\text{NH}_3\text{C}_6\text{H}_4\text{COOH})_3\text{H}_2\text{P}_3\text{O}_{10}$, are the same as those observed in the triphosphate associated to rubidium $\text{Rb}_3\text{H}_2\text{P}_3\text{O}_{10} \cdot 1,5\text{H}_2\text{O}$ ²²

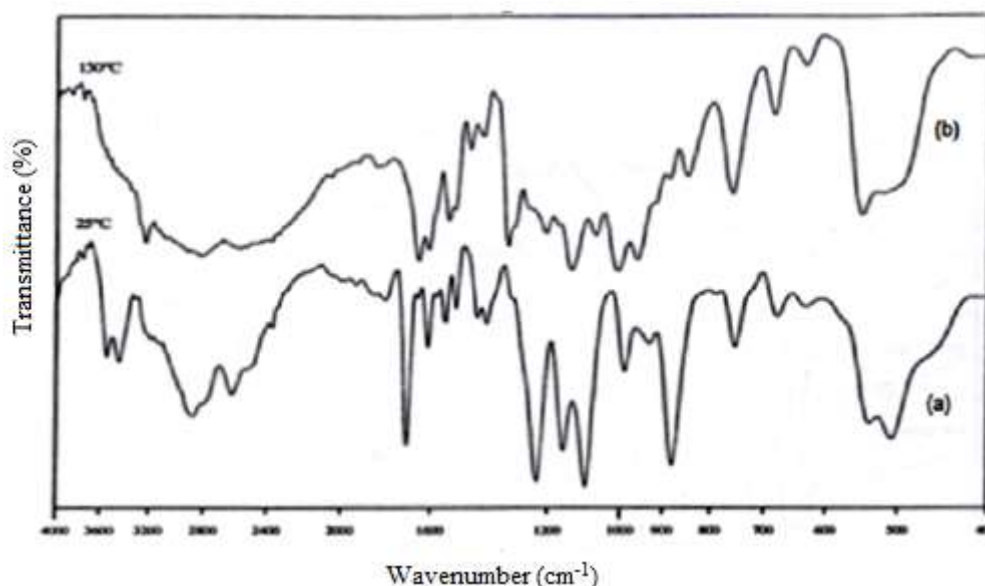


Figure 1. IR spectra of the phosphates: (a) $(\text{NH}_3\text{C}_6\text{H}_4\text{COOH})_3\text{H}_2\text{P}_3\text{O}_{10} \cdot 3\text{H}_2\text{O}$ and (b) $(\text{NH}_3\text{C}_6\text{H}_4\text{COOH})_3\text{H}_2\text{P}_3\text{O}_{10}$

Table 3. Characterization of $(\text{NH}_3\text{C}_6\text{H}_4\text{COOH})_3\text{H}_2\text{P}_3\text{O}_{10} \cdot 3\text{H}_2\text{O}$ and $(\text{NH}_3\text{C}_6\text{H}_4\text{COOH})_3\text{H}_2\text{P}_3\text{O}_{10}$ by IR vibration spectrometry ^{6, 12, 13}.

$\text{Rb}_3\text{H}_2\text{P}_3\text{O}_{10} \cdot 1,5\text{H}_2\text{O}$	$\text{NH}_2\text{C}_6\text{H}_4\text{COOH}$	$(\text{NH}_3\text{C}_6\text{H}_4\text{COOH})_3\text{H}_2\text{P}_3\text{O}_{10} \cdot 3\text{H}_2\text{O}$	$(\text{NH}_3\text{C}_6\text{H}_4\text{COO})_3\text{H}_2\text{P}_3\text{O}_{10}$	Vibrational modes
3553		3545		$\nu(\text{OH})$
3428	3466	3449		$\nu_{\text{as}}(\text{NH}_3^+)$
	3367			$\nu_{\text{as}}(\text{NH}_3^+)$
	3233		3230	
	3065			$\nu(\text{OH}) + \nu(\text{C-H})$
	2980	2885	2880	$\nu_{\text{s}}(\text{NH}_3^+)$
				Non-fundamental modes
2730			2780	
	2678	2614	2577	

2350	2552		2390	
			2036	
	1912			
			1846	β C=O in-plane
1770				
	1673	1698		δ (OH)/ ν C=O
	1632			
	1602	1614	1600	δ_{as} NH ₃ ⁺ / ν C=C/ ν C=O
	1580	1578	1561	δ_s NH ₃ ⁺ / ν C=C
	1532	1550	1539	δ_s NH ₃ ⁺ / ν C=C
		1510	1516	ν C=C
	1441	1431	1468	ν C-N/ β (OH)
	1420	1403	1424	ν C-N / β (OH)
	1321	1317	1341	ν C-C/ ν C-N/ ν C-O
	1293			
1233		1237		
1203				ν C-O/ β (C-H)/ β (P-OH)
1191	1180		1200	
		1156		
1126	1131		1130	β (C-H)/ ν (P=O)
1101		1096		β (C-H)/ ρ (NH ₃ ⁺)
	1075		1060	β (C-H)/ ρ (NH ₃ ⁺)
1032				β (C-H)
1000	970	997	1000	β (C-H) / ν C-O
	920	934	953	
	899	883	890	w(NH ₃ ⁺)/ ν PO ₂
	843		845	ν PO ₃
	773	761	756	δ (C-H)
714	709	727		ν P-O-P/ Ring breathing
684		686	678	t (NH ₃ ⁺)/ δ (C-H)
				δ (C-H)
	618	637		ν C=O
	555	542	540	ρ CO ₂ / ν PO ₄
	498	511		δ PO ₂

Study of the thermal behavior of (NH₄)₃P₃O₉

To facilitate the thermal behavior study of (NH₃C₆H₄COOH)₃H₂P₃O₁₀.3H₂O, we firstly studied the decomposition of (NH₄)₃P₃O₉, which was prepared by the method of ion-exchange resin⁹, and characterized crystallographically by M. Bagieu-Beucher in 1976²³. It crystallizes in the monoclinic system with space group P2₁/n (Z = 4) (C_{2h}⁵), and parameters: a = 11,515 Å, b = 12,206 Å, c = 7.699 Å, β = 101.63 °. The structure of (NH₄)₃P₃O₉ was resolved using that of its isotype K₃P₃O₉²³. In this structure, the P₃O₉ cycle does not have proper symmetry. Its C₁ symmetry is approximately C_{3v}, where k⁺ cations or NH₄⁺ occupy three separate sites.

Indeed, we have prepared (NH₄)₃P₃O₉ by the exchange resin method and controlled its purity by X-ray diffraction, and then we examine the thermal behavior, between 25 and 1400°C (sample mass: 23 mg) using the coupled TG-DTA analyses with a heating rate of 1°C/min. TGA, DTA and DTG curves

(Figures 2 and 3) show two distinct steps. The first step between 180°C and 450°C corresponds to a loss in brutal mass 17.5%. This loss is the equivalent of three ammonia molecules per formula unit. The DTG curve indicates two distinct peaks, the first at 180 °C and the second at 295°C. However, the elimination of the first molecule of NH₃ does not seem to be accompanied by a thermal effect. For the other two molecules of NH₃, the DTA curve indicates a peak, endothermic top temperature to 290°C, which is of asymmetrical profile. This confirms the existence of more than one type of site occupied by NH₄⁺ in the structure of (NH₄)₃P₃O₉. Moreover, explains the succeeding departure of 3 molecules of NH₃ because of distinct bond energies. At 450°C, after the departure of 3 ammonia molecules per formula unit and a thermal residue, 240 g/mol, destroyed (NH₄)₃P₃O₉ and leads to H₃P₃O₉. The reaction scheme is the following:

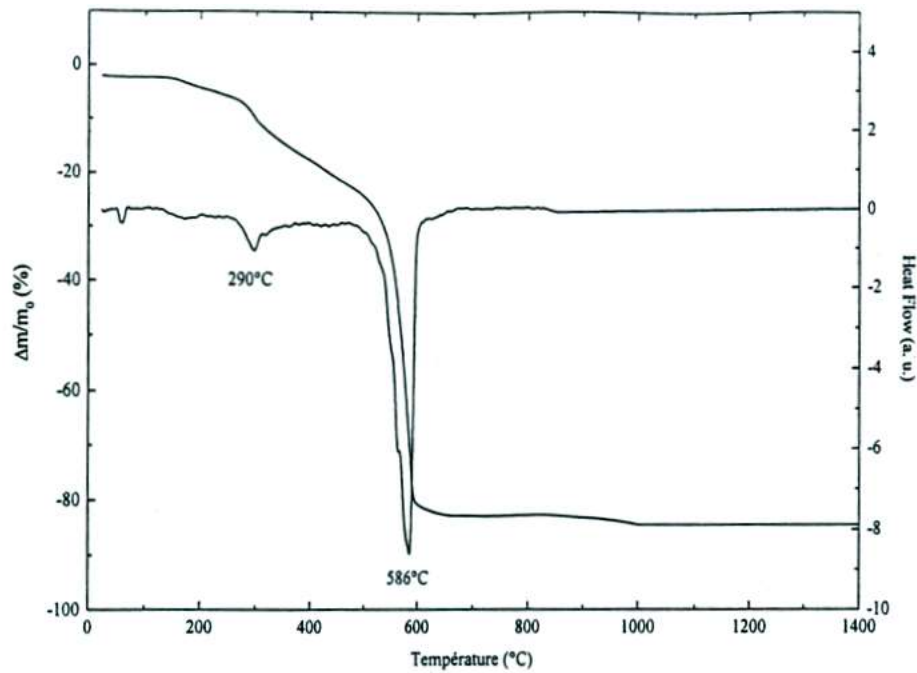


Figure 2. TGA-DTA thermograms of $(\text{NH}_4)_3\text{P}_3\text{O}_9$ ($V = 1^\circ\text{C}/\text{min}$).

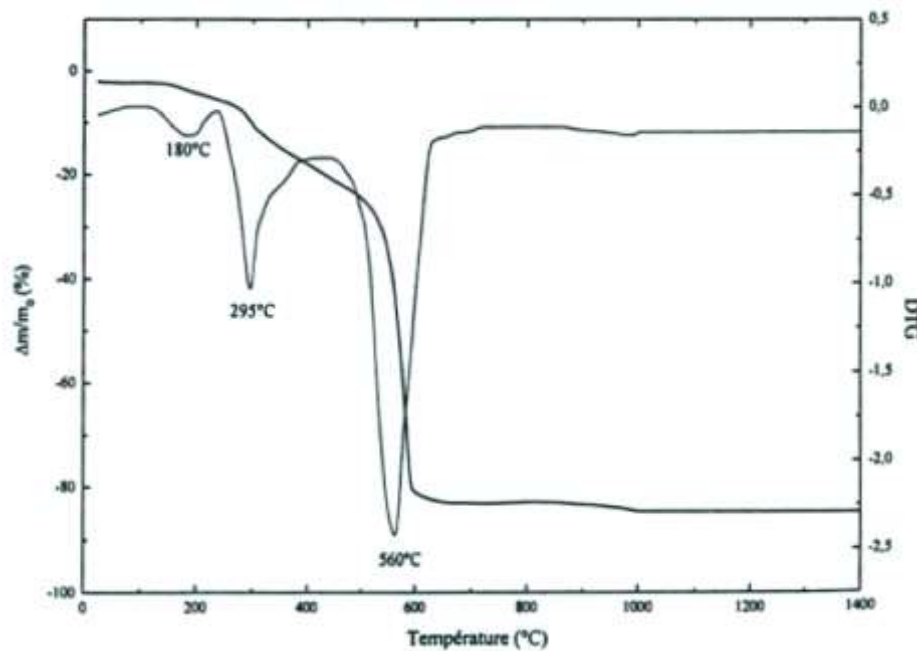
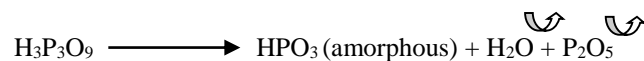


Figure 3. TG-DTG thermograms of $(\text{NH}_4)_3\text{P}_3\text{O}_9$ ($V = 1^\circ\text{C}/\text{min}$)

The second stage, between 450°C and 650°C , corresponds to a weight loss of 64.5%, the equivalent of $2/3$ of the weight of thermal residue $\text{H}_3\text{P}_3\text{O}_9$. This loss is accompanied by an intense and endothermic

DTA peak at 586°C due to the decomposition of the acid $\text{H}_3\text{P}_3\text{O}_9$ amorphous entity which releases H_2O and P_2O_5 with a top speed at 560°C on the DTG curve. At 650°C , the reaction scheme is the following:



Between 650°C and 1400°C , any mass loss was observed in the TGA thermogram, and any thermal

effect was highlighted by the TGA-DTA thermograms (Figure 2).

Study of the thermal behavior of $(\text{NH}_3\text{C}_6\text{H}_4\text{COOH})_3\text{H}_2\text{P}_3\text{O}_{10}\cdot 3\text{H}_2\text{O}$

The study of the thermal behavior of tetra (4-carboxyphenyl ammonium) dihydrogenotriphosphate trihydrate $(\text{NH}_3\text{C}_6\text{H}_4\text{COOH})_3\text{H}_2\text{P}_3\text{O}_{10}\cdot 3\text{H}_2\text{O}$, was performed by linear increase in temperature from 25 to 600°C using the TGA coupled on thermodifferential of powder samples of about 20 mg, at different heating rates: $v = 1, 3, 6, 10$ and 15°C/min under atmospheric pressure.

Thermogravimetric analysis

The TGA thermograms of $(\text{NH}_3\text{C}_6\text{H}_4\text{COOH})_3\text{H}_2\text{P}_3\text{O}_{10}\cdot 3\text{H}_2\text{O}$, realized at different heating rates (Figure 4), have all the same look and show five separate mass loss steps. Careful examination of the thermograms, carried out at low speed, indicates that the first step is not on that initially the water whereas the other four steps are related to entities from the decomposition of the organic matrix and the mineral matrix.

The TGA-DTA thermogram realized at a heating rate of 3°C/min (Figure 5) shows 5 mass loss steps:

- The first stage begins at 110°C and ends at 126°C. It appears to involve a single process of evolving water (mass loss calculated 7.47%, observed 7.5%). The

DTG thermogram has a maximum loss of water at 118°C.

Between 126 and 168°C, in the TGA thermogram, there is no variation of mass.

- The second step starts at 168°C and ends at 188°C. It corresponds to a mass loss, relatively fast, about 7.01%. It is attributed to the loss of three molecules of ammonia for which the loss mass is theoretically calculated of 7.05%. The maximum loss is observed on the DTG thermogram at 179°C.

- The third stage, between 188 and 260°C, corresponding to a mass loss of 18.22%, is assigned to 3 moles of CO_2 per formula unit (mass loss calculated 18.2%). Two loss maxima are reported on the DTG curve, during the third step, the first peak well pronounced at 197°C and a second peak doubtful to 214°C.

- The fourth step starts at 260 and ends at 310°C. It corresponds to a weight loss of 13.4% and could be attributed to the loss of gas from the decomposition of the residual heat. The maximum rate of loss is observed on the DTG thermogram at 280°C.

- The fifth stage, between 310 and 530°C, corresponding to a mass loss of 20.9%. This loss could be attributed to the combustion of the organic matrix.

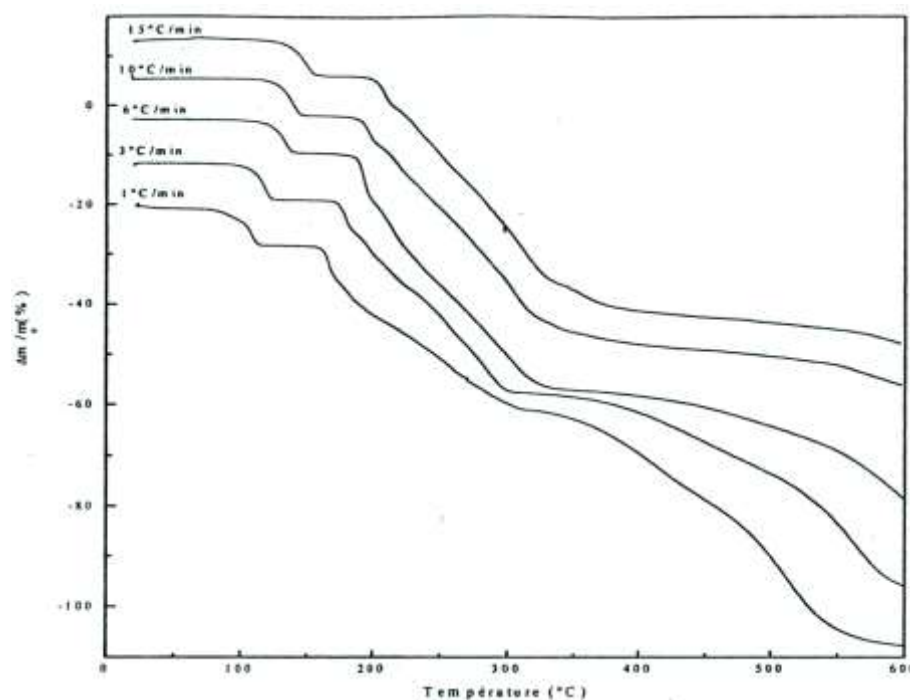


Figure 4. TGA thermograms of $(\text{NH}_3\text{C}_6\text{H}_4\text{COOH})_3\text{H}_2\text{P}_3\text{O}_{10}\cdot 3\text{H}_2\text{O}$ at different heating rates.

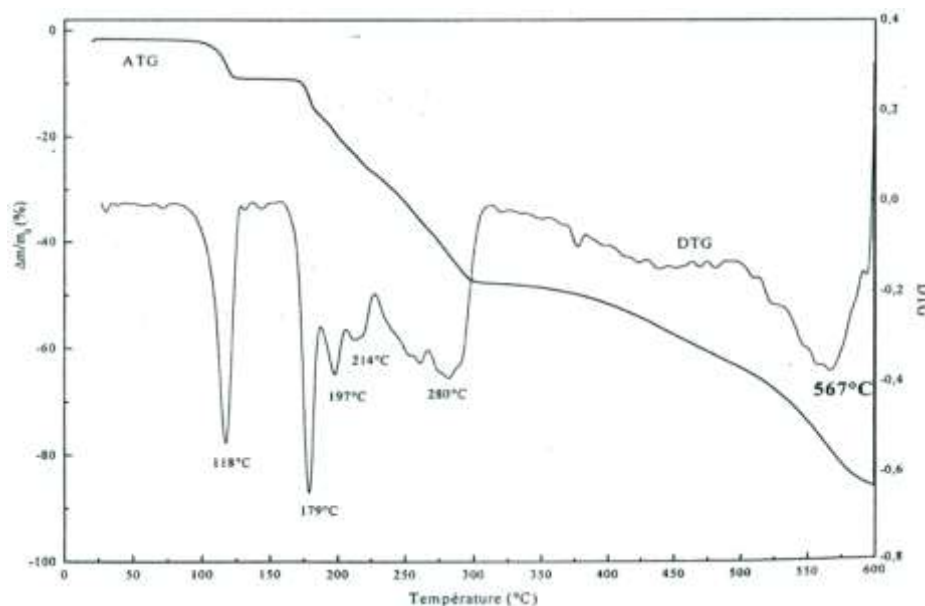
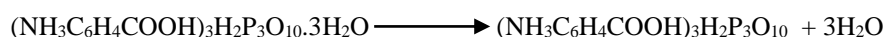


Figure 5. TG-DTG thermograms of $(\text{NH}_3\text{C}_6\text{H}_4\text{COOH})_3\text{H}_2\text{P}_3\text{O}_{10}\cdot 3\text{H}_2\text{O}$ at $3^\circ\text{C}/\text{min}$.

- The sixth stage, between 530 and 600°C , corresponding to a weight loss of 17%, is accompanied by a DTG peak at 567°C corresponding to the maximum speed of water H_2O and pentoxide phosphorus P_2O_5 release from the decomposition of the mineral matrix.

Differential thermal analysis

DTA thermograms made at different speeds and coupled with the thermogravimetric analysis are



An exothermic peak was observed at 147°C only for the weak heating rates for 1 and $3^\circ\text{C}/\text{min}$ after the total removal of water. It corresponds to the crystallization of the corresponding anhydrous $(\text{NH}_3\text{C}_6\text{H}_4\text{COOH})_3\text{H}_2\text{P}_3\text{O}_{10}$. This well-crystallized phase was characterized by its IR spectrum (Figure 1).

- The second stage, between 168 and 188°C , is accompanied by two endothermic peaks at 174 and 180°C . The last peak at 180°C coincides with the maximum loss at 179°C . These two endothermic



- The third stage, between 188 and 260°C , corresponding to the departure of 3 moles of CO_2 , is accompanied by an endothermic peak at 197°C which coincides with the maximum loss reported on the DTG curve peak at 197°C . It is worth noticing that this third stage can be subdivided into two distinct stages. The first one is made between 188 and 210°C , the second between 210 and 260°C . In this case, the endothermic peak observed at 197°C would be the CO_2 group the more weakly bonded to the organic chain



shown in Figure 6. The analysis of the thermogram corresponding to the heating rate $3^\circ\text{C}/\text{min}$ (Figure 7) allows to highlight the following points:

The first phase, between 110 and 126°C , accompanied by an endothermic peak at 118°C , which coincides with the maximum reported loss on the derivative curve at 118°C . This peak corresponds to the loss of 3 water molecules according to the following reaction scheme:

effects are attributed to the loss of three molecules of ammonia. The presence of two endothermic peaks may be interpreted based on structural data of $(\text{NH}_3\text{C}_6\text{H}_4\text{COOH})_3\text{H}_2\text{P}_3\text{O}_{10}\cdot 3\text{H}_2\text{O}$, which indicates the presence of three types of nitrogen atoms. The first endothermic peak at 174°C , can be attributed to the departure of two moles of ammonia NH_3 (1) and NH_3 (3), the two nitrogen atoms having thermal agitation factors very close ^{2,7}, and the second at 180°C , the last remaining ammonia molecule NH_3 (2) (having a nitrogen atom of thermal agitation factor low ¹²). The reaction scheme is as follows:

The endothermic peak observed at 197°C is related to the CO_2 group, more weakly bonded to the organic chain (CO_2 (7)), and it corresponds to the liberation of 6.06%, the CO_2 removed between (1/3) 188 and 210°C (18.02%). The second stage from 12.1% per formula unit; (2/3) of CO_2 corresponding to groups (CO_2 (14)) and (CO_2 (21)). Indeed, the structure of the compound shows that the C_6 - C_7 distance is relatively longer, 1.498\AA longer, longer than 1.498\AA . The reaction scheme in this step is as follows:

The thermal residue obtained at the end of the third stage ($(C_6H_5)_3H_2P_3O_{10}$) after loss successively of 3 H_2O , ($2NH_3$, $1NH_3$) and 3 CO_2 per formula unit undergoes thermal degradation of organic matrices and mineral. The ATD Thermogram brings up an exothermic peak at around $300^\circ C$, which could be attributed to an atomic reorganization. Indeed, the temperature of the start of the exothermic effect

coincides with the onset temperature of the 4th stage and the exothermic peak observed at $300^\circ C$ corresponds to the temperature of the end of this step.

- The fifth stage, between 310 and $530^\circ C$, make appear an exothermic peak at the top temperature of $432^\circ C$, which may be due to the burning of the residue of the organic matrix.

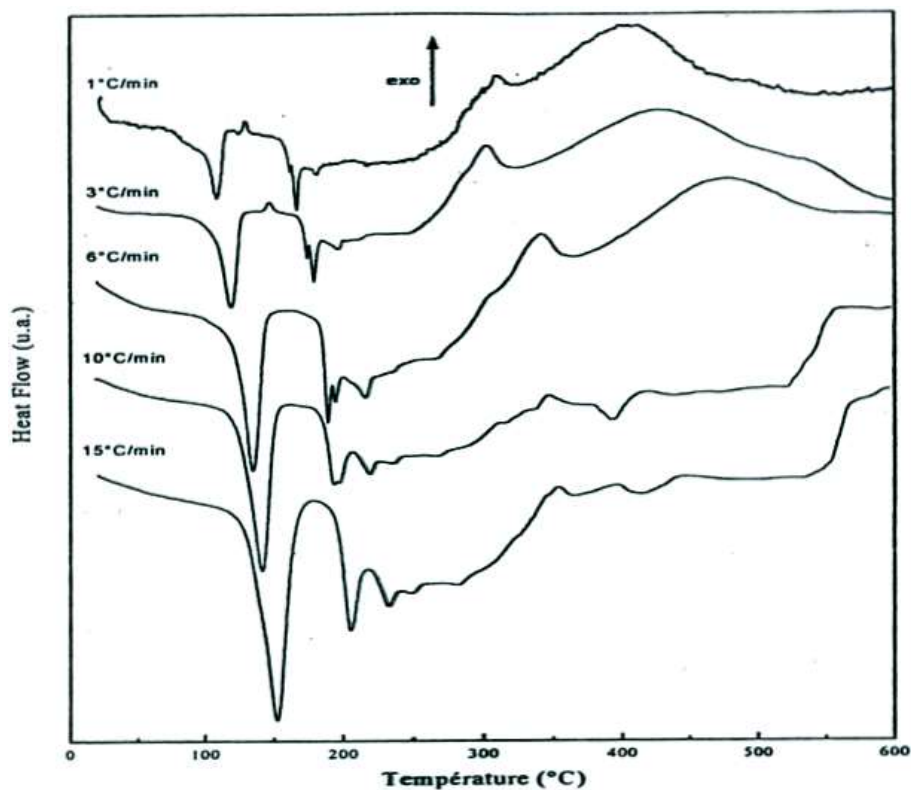


Figure 6. TGA thermograms of $(NH_3C_6H_4COOH)_3H_2P_3O_{10}.3H_2O$ at different heating rates

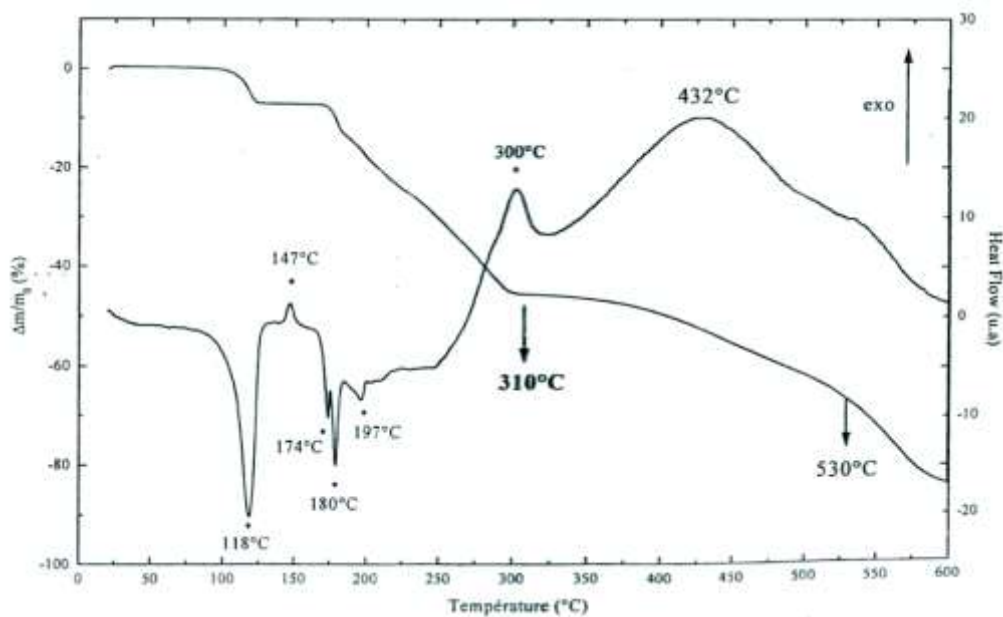


Figure 7. TGA-DTA thermograms of $(NH_3C_6H_4COOH)_3H_2P_3O_{10}.3H_2O$ at $3^\circ C/min$.

Measurement of kinetic parameters

Estimation of the thermodynamic functions: Various equations of kinetic analyses are known ²³⁻²⁷.

Ozawa and KAS methods are selected in studying the kinetics of thermal dehydration of the title compound. So, water loss kinetic parameters were evaluated from

the curves $\ln(v/T^2m) = f(1/Tm)$ and $\ln(v) = f(1/Tm)$ (Figures 8 and 9), where (v) is the heating rate and T_m the sample temperature at the thermal effect maximum. The characteristic temperatures at

maximum dehydration rates, T_m in °C, at different heating rates from the DTA curves of $(NH_3C_6H_4COOH)_3H_2P_3O_{10} \cdot 3H_2O$ are gathered in Table 4.

Table 4. Temperatures of endothermic peak summits on the DTA curves of $(NH_3C_6H_4COOH)_3H_2P_3O_{10} \cdot 3H_2O$.

heating rates	1°C/min	3°C/min	6°C/min	10°C/min	15°C/min	Temperatures of endothermic peak summits (°C)
3 H ₂ O	108	118	134	142	152	
2 NH ₃	161.4	174	189	193.4	206	
1 NH ₃	166.6	180	194	198	206	
3 CO ₂	181.6	197	216	219	233	

From these temperatures, the apparent activation energies of dehydration were calculated for the $(NH_3C_6H_4COOH)_3H_2P_3O_{10} \cdot 3H_2O$. For the Kissinger-Akahira-Sunose (KAS) ²⁶ method, the slope of the resulting straight line of the curve: $\ln(v/T^2m) = f(1/Tm)$ (Figure 8), equals to :

$-E_a/R$ allows the apparent activation energy to be calculated (Table 4). With reference to the Ozawa method, the slope of the resulting straight line on the curve: $\ln(v) = f(1/Tm)$ (Figure 9), equals to $-1.0516E/R$, also allows the apparent activation energy to be calculated by this second way (Table 4). The equations used for the two methods are the following:

for KAS ²⁷

$$\ln\left(\frac{v}{T^2m}\right) = \ln\left(\frac{AR}{E}\right) - \left(\frac{E}{R}\right)\left(\frac{1}{T_m}\right) \quad (1)$$

for Ozawa ²⁷

$$\ln(v) = \ln\left(\frac{AR}{1.0516E}\right) - 1.0516\left(\frac{E}{R}\right)\left(\frac{1}{T_m}\right) \quad (2)$$

The pre-exponential factor or Arrhenius constant (A) and the related thermodynamic functions can be calculated by using the activated complex theory (transition state) of Eyring ²⁹⁻³¹. The following general equation can be written ³¹:

$$A = \left(\frac{e\chi k_B T_m}{h}\right) \exp\left(\frac{\Delta S^*}{R}\right) \quad (3)$$

Where e is the Neper number ($e = 2.7183$), χ is the transition factor, which is unity for the monomolecular reaction, k_B is the Boltzmann constant ($k_B = 1.3806 \times 10^{-23}$ J K⁻¹), h is Plank's constant ($h = 6.6261 \times 10^{-34}$ J s), T_m is the peak temperature of the DTA curve, R is the gas constant ($R = 8.314$ J

K⁻¹ mol⁻¹) and ΔS^* is the entropy change of transition state complex or entropy of activation. Thus, the entropy of activation may be calculated as follows:

$$\Delta S^* = R \ln \frac{Ah}{e\chi k_B T_m} \quad (4)$$

The enthalpy change of transition state complex or heat of activation (ΔH^*) and Gibbs free energy of activation (ΔG^*) of decomposition were calculated according to Eqs. (5) and (6), respectively:

$$\Delta H^* = E^* - R T_m \quad (5)$$

$$\Delta G^* = \Delta H^* - T_m \Delta S^* \quad (6)$$

Where, E^* is the activation energy E_a of both KAS ²⁵ and Ozawa ²⁶ methods. The values of the activation energy are gathered in (Table 5). Thermodynamic functions were calculated from Eqs. (4), (5) and (6) and summarized in (Table 6). The negative values of ΔS^* from two methods for the dehydration step reveals that the activated state is less disordered compared to the initial state. These ΔS^* values suggest a large number of degrees of freedom due to rotation which may be interpreted as a « slow » stage ³⁰⁻³³ in this step. The positive values of ΔG^* at all studied methods are because, the dehydration processes are not spontaneous. The positivity of ΔG^* is controlled by a small activation entropy and a large positive activation enthalpy according to the Eq. 6. The endothermic peaks in DTA data agree well with the positive sign of the activation enthalpy (ΔH^*). The estimated thermodynamic functions ΔS^* and ΔG^* (equation 6, Table 6) from two methods are approximatively the same due to the same pre-exponential factor of about 10^{12} . While ΔH^* (equation 5, Table 6) exhibits, in all the cases, an independent behavior on the pre-exponential factor as seen from exhibiting nearly the same value.

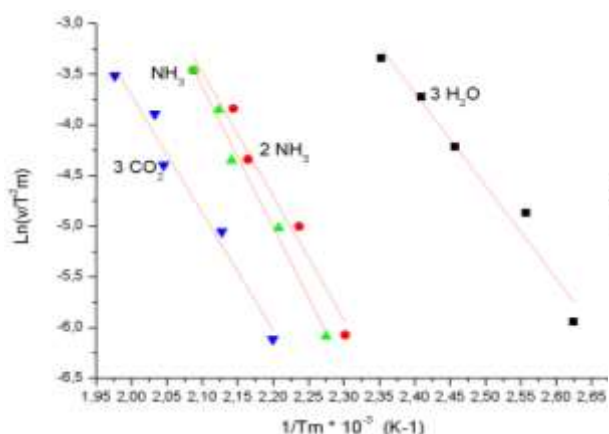


Figure 8. Straight $\text{Ln}(v/T^2m) = f(1/Tm)$ of $(\text{NH}_3\text{C}_6\text{H}_4\text{COOH})_3\text{H}_2\text{P}_3\text{O}_{10} \cdot 3\text{H}_2\text{O}$

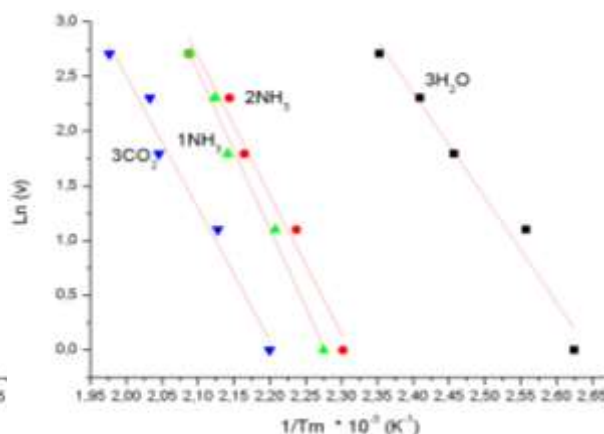


Figure 9. Straight $\text{Ln}(v) = f(1/Tm)$ of $(\text{NH}_3\text{C}_6\text{H}_4\text{COOH})_3\text{H}_2\text{P}_3\text{O}_{10} \cdot 3\text{H}_2\text{O}$

Table 5. Activation energy values E_a , pre-exponential factor (A) and correlation coefficient (r^2) calculated by Ozawa and KAS methods for the dehydration of $(\text{NH}_3\text{C}_6\text{H}_4\text{COOH})_3\text{H}_2\text{P}_3\text{O}_{10} \cdot 3\text{H}_2\text{O}$ under atmospheric pressure.

Steps	OZAWA			K.A.S		
	E_a (kJ/mol)	A (min^{-1})	r^2	E_a (kJ/mol)	A (min^{-1})	r^2
Step 1 (3H ₂ O)	75.6954	2.3714×10^{12}	0.97	76.2636	8.3937×10^{11}	0.963
Step 2 (2NH ₃)	99.9956	7.8151×10^{12}	0.973	101.373	6.6787×10^{12}	0.97
Step 3 (1NH ₃)	112.9685	4.3858×10^{12}	0.99	114.992	3.6930×10^{12}	0.99
Step 4 (3CO ₂)	92.9084	3.9084×10^{12}	0.971	96.1057	3.0864×10^{12}	0.97

Table 6. Values of ΔS^\ddagger , ΔH^\ddagger and ΔG^\ddagger for dehydration step of $(\text{NH}_3\text{C}_6\text{H}_4\text{COOH})_3\text{H}_2\text{P}_3\text{O}_{10} \cdot 3\text{H}_2\text{O}$ calculated according to Ozawa and KAS equations.

Steps	OZAWA			K.A.S		
	ΔS ($\text{J} \cdot \text{K}^{-1} \cdot \text{mol}^{-1}$)	ΔH ($\text{kJ} \cdot \text{mol}^{-1}$)	ΔG ($\text{kJ} \cdot \text{mol}^{-1}$)	ΔS ($\text{J} \cdot \text{K}^{-1} \cdot \text{mol}^{-1}$)	ΔH ($\text{kJ} \cdot \text{mol}^{-1}$)	ΔG ($\text{kJ} \cdot \text{mol}^{-1}$)
Step 1 (3H ₂ O)	-19.2678	72.1619	80.3508	-27.9027	72.7302	84.5888
Step 2 (2NH ₃)	-10.3472	96.0132	100.969	-11.4960	97.4661	102.869
Step 3 (1NH ₃)	-15.1501	108.98614	116.2431	-16.5795	111.0096	118.9513
Step 4 (3CO ₂)	-16.5641	91.0571	99.4386	-18.5271	91.8983	101.273

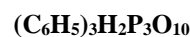
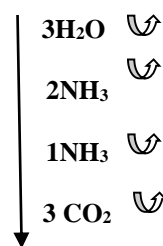
Conclusion

The structural and thermal study of 4-carboxyphenyl dihydrogenotriphosphate ammonium trihydrate $(\text{NH}_3\text{C}_6\text{H}_4\text{COOH})_3\text{H}_2\text{P}_3\text{O}_{10} \cdot 3\text{H}_2\text{O}$ developed by IR spectrometry vibration and TGA-DTA analyses coupled brings up the following results:

The reaction of phosphoric acid with aminobenzoic acid leads, due to the hydrolysis of $\text{P}_3\text{O}_9^{3-}$ ion in aqueous solution or by using $\text{H}_5\text{P}_3\text{O}_{10}$, to a triphosphate with a formula $(\text{C}_7\text{H}_8\text{NO}_2)_3\text{H}_2\text{P}_3\text{O}_{10} \cdot 3\text{H}_2\text{O}$. The structural resolution shows the existence of ion channels $\text{H}_2\text{P}_3\text{O}_{10}^{3-}$ linked

together by hydrogen bonds. Organic cations, water molecules and phosphates chains are linked together by hydrogen bonds. A detailed vibrational study is reported for $(\text{NH}_3\text{C}_6\text{H}_4\text{COOH})_3\text{H}_2\text{P}_3\text{O}_{10} \cdot 3\text{H}_2\text{O}$ with all of its entities NH_3 , $\text{C}_6\text{H}_4\text{COOH}$, $\text{H}_2\text{P}_3\text{O}_{10}$ and H_2O . The thermal analysis showed that the compound is stable between 25 and 90°C and has confirmed the number of water molecules per formula unit. This loss of water takes place in one step and leads to the crystallization of the anhydrous phase, $(\text{C}_7\text{H}_8\text{NO}_2)_3\text{H}_2\text{P}_3\text{O}_{10}$, which was characterized by its X-ray powder diffraction pattern and IR spectrum. This phase $(\text{C}_7\text{H}_8\text{NO}_2)_3\text{H}_2\text{P}_3\text{O}_{10}$ was found stable in a small temperature range, 150-160°C. We have shown that by raising the temperature, the anhydrous phase

loses successively 3H₂O ((2) NH₃, (1) NH₃) and 3CO₂ per formula unit. For each of these entities released, the apparent activation energy was measured. These energies are respectively 73,4 kJ/mol for 1 NH₃ and 92,29 kJ/mol for 3CO₂. Between 260 and 300°C, the residual mass, (C₆H₅)₃H₂P₃O₁₀ undergoes a weight loss corresponding to a molar loss of 70 g/mol. This weight loss is accompanied by an atomic rearrangement which results on the DSC thermogram with a peak at 300°C. Beyond 300°C, there is degradation of the organic matrix and / or the mineral matrix. An exothermic peak at the top temperature at 432°C could be the combustion of the residue of the organic matrix.



References

- 1- S.I. Akberova, New Biological Properties of *p*-aminobenzoic Acid Biol Bull Russian Acad Sci., **2002**, 29: 390-393.
- 2- N. Benali-Cherif, F. Allouche, A. Direm, and K. Soudani, Hydrogen bonding in 2-carboxyanilinium dihydrogen phosphite at 100 K, Acta Cryst E, **2009**, E65, 0064-0065
- 3- N. Benali-Cherif, F. Allouche, A. Direm, and K. Soudani, Hydrogen bonding in 4-carboxyanilinium Dihydrogenphosphate, Acta Cryst E, **2007**, E63, 02272-02274
- 4- N. Benali-Cherif, F. Allouche, A. Direm, and K. Soudani, 4-Carboxyanilinium hydrogensulfate, Acta Cryst E, **2007**, E63, 02054-02056
- 5- N. Benali-Cherif, A. Abouimrane, K. Sbai, H. Merazig, A. Cherouana and L. Bendjeddou, *p*-Carboxyphenylammonium dihydrogenmonophosphate Monohydrate, Acta Cryst E, **2002**, E58, 0160-0161
- 6- J. Chékir-Mzali, S. Elgharbi, K. Horchani-Naifer, M. Ferid, Synthesis, vibrational characteristic and luminescence properties of Er³⁺ in HNH₄ErP₃O₁₀, Optical Materials, **2017**, 37, 188
- 7- A. Charaf, I. Fahim, EL. M. Tace, M. Tridane, M. Radid and S. Belaouad, Physico-chemical studies of CuNa₃P₃O₁₀·12H₂O, crystallographic characterization of CuNa₃P₃O and quantum chemical calculations of The PO₁₀⁵⁻ ion, Phosphorus Research Bulletin, **2010**, 24, 83.
- 8- I. Fahim, A. Kheireddine, M. Tridane, and S. Belaouad, Chemical preparation and XRD data for a new triphosphate CuNaP₃O₁₀ and two cyclotriphosphates SrRbP₃O₉·3H₂O and SrRbP₃O₉, Powder Diffraction, **2011**, 26 (1), 78-81.
- 9- I. Fahim, M. Tridane and S. Belaouad, Physico-chemical studies of MgNa₃P₃O₁₀·12H₂O, XII^{ème} Rencontre Marocaine sur la Chimie de l'Etat Solide (REMCES XII), MATEC Web of Conferences, **2013**, 5, 04035.
- 10- M. Tridane, I. Fahim, S. Benmokhtar and S. Belaouad, Structural modifications from NiNa₃P₃O₁₀·12H₂O to NiNa₃P₃O₁₀ new triphosphate during the dehydration process, Phosphorus Research
- 11- A. Jouini and A. Durif, Utilisation des résines dans la préparation des phosphates condensés, C R Acad Sci., **1983**, 297 II, 573-578,
- 12- M. Belhabra, S. Zerraf, A. Kheireddine, K. El Kababi, A. atibi, M. tridane, M. Radid, and S. Belaouad, Chemical preparation and crystallographic characterization of BaCsP₃O₉·2H₂O, (NH₃C₆H₄COOH)₃H₂P₃O₁₀·3H₂O and it is corresponding anhydrous, (NH₃C₆H₄COOH)₃H₂P₃O₁₀, Am. J. innov. res. Appl. sci., **2017**, 4(6), 223-229.
- 13- K. El Kababi, A. atibi, R. Lamsatfi, S. Zerraf, I. Fahim, M. Tridane and S. Belaouad, Chemical Preparation, XRD Data and IR Studies for an Organic Triphosphate and Its Anhydrous New Form (NH₃C₆H₄COOH)₃H₂P₃O₁₀, International Journal of Trend in Research and Development, **2016**, 3(3), 302-305.
- 14- I. Fahim, A. Kheireddine, S. Belaouad, Sodium tripolyphosphate (STPP) as a novel corrosion inhibitor for mild steel in 1 M HCl, Journal of Optoelectronics and Advanced Materials, **2013**, 15(5-6), 451
- 15- A. Kheireddine, M. Tridane and S. Belaouad, Chemical preparation, the kinetics of thermal behavior and infrared studies of Pb₃(P₃O₉)₂·3H₂O and Cd₃(P₃O₉)₂·14H₂O, Mediterr. J. Chem., **2013**, 2(4), 549-568
- 16- A. Atibi, K. El Kababi, M. Belhabra, S. Zerraf, M. Tridane & S. Belaouad, Chemical preparation, crystal structure and vibrational study of a new dihydrogenotriphosphate trihydrate of 4-aminobenzoic acid fertilizer type NP, Journal of Coordination Chemistry, **2018**, 71(21), 3510-3520
- 17- M. Samsonowicz, T. Hrynaszkiwicz, R. Swislocka, W. Lewandowski, Experimental and theoretical IR, Raman, NMR spectra of 2-, 3- and 4-aminobenzoic acids, Journal of Molecular Structure, **2005**, 744, 345-352

MEDITERRANEAN JOURNAL OF CHEMISTRY

- 18- J. Antony, GV. Helden, G. Meijer, B. A. Schmidt, Anharmonic midinfrared vibrational spectra of benzoic acid monomer and dimer, *J Chem Phys*, **2005**, 123, 014305
- 19- G.M. Florio, T.S. Zwier, E.M. Myshakin, K.D. Jordan, and E.L. Sibert III, Theoretical modeling of the OH stretch infrared spectrum of carboxylic acid dimers based on first-principles anharmonic couplings, *J. Chem. Phys.*, **2003**, 118, 1735
- 20- Ch. Muthuselvi, A. S. Princy and S. S. Pandiarajan, Growth and Characterization of 4-carboxyanilinium Dihydrogen Phosphate Semi-Organic Complex Crystal, *Asian J Applied Sc.*, **2017**, 10(4), 159-169
- 21- Abraham F. Jalbout, Zhen-Yi Jiang, A. Ouasri, H. Jeghnou, A. Rhandour, M. C. Dhamelincourt, P. Dhamelincourt, A. Mazzah, Theoretical and experimental vibrational analysis of $[C_6H_5NH_3]_2SiF_6$, *J Vibrational Spectroscopy*, **2003**, 33, 21-30
- 22- V. Koval, P. Nagorny, Effect of addition of ammonium dihydrophosphate on the formation of insoluble polyphosphates by condensation of potassium dihydrophosphate at 225°C, *J Appl chem.*, **1990**, 62, 2373
- 23- M. Bagieu-Beucher, I. Tordjman, A. Durif and J. Guitel, Structure Crystalline du Trimétaphosphate de Potassium $K_3P_3O_9$, *Acta Crystallogr.*, **1976**, B32, 1427-1430
- 24- H. E Kissinger, Reaction Kinetics in Differential Thermal analysis, *Anal. Chem.*, **1957**, 29, 1702
- 25- T. Akahira and T. Sunose, "Transactions joint convention of four electrical institutes, paper no. 246 (1969) research report, Chiba Institute of Technology," *Journal of Science Education and Technology*, **1971**, 16, 22-31.
- 26- T. A Ozawa, A New Method of Analyzing Thermogravimetric Data, *Bull Chem Soc Jpn*, **1965**, 38, 1881-1886.
- 27- A. W. Coats, J. P. Redfern, Kinetic Parameters from Thermogravimetric Data, *Nature*, **1964**, 201, 68-69.
- 28- D. W. Van Krevelns, P.J. Hoftijzer, Kinetics of gas-liquid reaction-general theory, *Trans I Chem*, **1954**, E 32, 5360
- 29- V. Šatava F. Škvára, Mechanism and Kinetics of the Decomposition of Solids by a Thermogravimetric Method, *J. Am. Ceram. Soc.*, **1969**, 52(11), 591-595.
- 30- J. Rooney, J. Eyring, Eyring transition-state theory and kinetics in catalysis, *J Mol Catal A Chemical*, 1995, 96, L1-L3.
- 31- B. Boonchom, Kinetics and Thermodynamic Properties of the Thermal Decomposition of Manganese Dihydrogenphosphate Dihydrate, *J Chem Eng Data*, **2008**, 53, 1533-1538.
- 32- L. Valaev, N. Nedelchev, K. Gyurova, M. Zagorcheva, A comparative study of non-isothermal kinetics of decomposition of calcium oxalate monohydrate, *J Anal Appl Pyrol*, **2008**, 81, 253-262.
- 33- P. Noisong, C. Danavirutai, T. Boonchom, Synthesis, characterization and non-isothermal decomposition kinetics of manganese hypophosphite monohydrate, *Solid State Sci*, **2008**, 10, 1598-1604.